

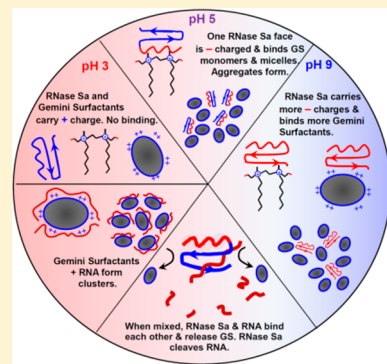
Gemini Surfactants Affect the Structure, Stability, and Activity of Ribonuclease Sa

Razieh Amiri,[†] Abdol-Khalegh Bordbar,[†] and Douglas V. Laurents*,[‡]

[†]Department of Chemistry, University of Isfahan, Isfahan 81746-73441, Iran

[‡]Rocasolano Institute of Physical Chemistry (IQFR/CSIC), Serrano 119, E-28006, Madrid, Spain

ABSTRACT: Gemini surfactants have important advantages, e.g., low micromolar CMCs and slow millisecond monomer ↔ micelle kinetics, for membrane mimetics and for delivering nucleic acids for gene therapy or RNA silencing. However, as a prerequisite, it is important to characterize interactions occurring between Gemini surfactants and proteins. Here NMR and CD spectroscopies are employed to investigate the interactions of cationic Gemini surfactants with RNase Sa, a negatively charged ribonuclease. We find that RNase Sa binds Gemini surfactant monomers and micelles at pH values above 4 to form aggregates. Below pH 4, where the protein is positively charged, these aggregates dissolve and interactions are undetectable. Thermal denaturation experiments show that surfactant lowers RNase Sa's conformational stability, suggesting that surfactant binds the protein's denatured state preferentially. Finally, Gemini surfactants were found to bind RNA, leading to the formation of large complexes. Interestingly, Gemini surfactant binding did not prevent RNase Sa from cleaving RNA.



INTRODUCTION

Currently, there is a need for improved surfactants for industrial, medical, and scientific applications. Moreover, in biochemical research, the isolation and characterization of membrane proteins and their interactions with other biomolecules represents an important challenge. These studies usually employ conventional surfactants consisting of a single hydrocarbon tail to bind to the hydrophobic surface of the membrane protein and a single polar headgroup to achieve solubility in aqueous solution. Early research on these simple surfactants elucidated the physical chemical basis for their formation^{1,2} and uncovered how the length of the hydrophobic tail and the presence of other amphiphiles affect the critical micelle concentrations (CMCs), aggregation number, and shape of micelles.^{2–4} This work also lent insight into surfactant behavior in practical applications, such as SDS-PAGE to determine protein molecular weights.⁵ However, these simple surfactants often present experimental problems due to their high CMCs, fast monomer micelle kinetics, and the need to employ high concentrations of deuterated surfactants for liquid state NMR studies. Moreover, membrane proteins can become inactive when their substrates and cofactors are trapped inside the surfactant micelles. To surmount these problems, new types of improved surfactants are being designed and tested. For example, amphilipids, a class of designed surfactants with dispersed hydrophobic groups and a reduced capacity to form micelles, have successfully kept membrane proteins soluble and stable in aqueous solution.⁶ However, amphilipids are rather difficult to prepare and purify.

Gemini surfactants are composed of two hydrophobic tails and two polar head groups connected by a linker.⁷ Gemini

surfactants have potential advantages for biochemical studies including low, micromolar CMCs, slow, millisecond monomer ↔ micelle kinetics, and relatively facile synthesis and purification. In industrial applications, their low CMC means that small amounts of Gemini surfactants can replace large amounts of conventional surfactants, providing significant cost and environmental benefits.⁸ For biochemical research, the low CMCs of Gemini surfactants permit experiments to be done at surfactant concentrations around 1 mM, as compared to 20 or 40 mM for conventional surfactants, which eliminates the need for deuteration for NMR experiments. Moreover, the much lower concentration of micelles formed should minimize the trapping of nonpolar cofactors and substrates.

To fully comprehend the factors influencing Gemini surfactant self-assembly, the contribution of the length⁹ and polarity¹⁰ of the spacer group or the addition of related simple surfactants to form mixed micelles¹¹ on the CMC, internal viscosity, aggregation number, and shape have been thoroughly investigated, and revealed the importance of the hydrophobic spacers' length. A careful analysis of a series of surfactants with the same aliphatic tail but one, two, and three charged head groups unveiled trends toward smaller, more spherical, and less tightly packed micelles as the number of charges on the headgroup increases.¹² Substitution of the typical Gemini surfactant counterion Br⁻ for the fatty acid C₁₅H₃₃CO₂⁻ led to the formation of vesicle structures¹³ which were meticulously characterized.¹⁴

Received: May 8, 2014

Revised: August 1, 2014

Published: August 18, 2014



More recently, the knowledge gained from this fundamental research has been applied toward solving nanotechnological and medical problems. For example, the length of the spacer also proves crucial for the ability of Gemini surfactants with ammonium or imidazolium head groups to modulate the growth of silver nanorods¹⁵ or 2D Langmuir films,¹⁶ respectively. When mixed with zwitterionic lipids carrying two aliphatic tails, Gemini surfactants bearing cholesterolic tails and ammonium groups form promising vehicles for gene delivery.¹⁷ Optimally, the proportion of Gemini surfactant should be kept low to reduce cytotoxicity yet be high enough to endow the whole surfactant + DNA complex with a net positive charge, which is necessary for efficient interaction with the target cell membrane.¹⁸ It has also been found that Gemini surfactants with shorter spacers showed higher transfection efficiencies.¹⁹ Very recently, Gemini surfactants bearing cholesterolic tails and imidazolium head groups have been utilized to introduce enhanced green fluorescent protein–pS3 conjugates into cancer cells, leading to the successful induction of apoptosis in cultured cancer cells as well as in tumors transplanted onto nude mice,²⁰ at efficiencies superior to those afforded by currently available commercial products.

As described above, for NMR structural studies using surfactant micelles as membrane mimetics, it is important that the CMC be as low as possible. Therefore, we have chosen to utilize the series of 16-s-16 MEA Gemini surfactants, with “s” being the number of $-\text{CH}_2-$ moieties in the linker, originally developed by Devi and co-workers,²¹ in which one methyl moiety ($-\text{CH}_3$) in each of the two head groups has been replaced by an ethanol moiety ($-\text{CH}_2-\text{CH}_2-\text{OH}$). These substitutions lower the CMCs 10-fold. This order-of-magnitude reduction of the CMC was attributed to improved solvent shielding of the aliphatic groups by the ethanol moiety which leads to an increased stabilizing contribution from the hydrophobic effect.²¹ Devi and co-workers studied 16-s-16 MEA Gemini surfactants with “s” = 4, 6, 8, and 10 and reported weak spacer length effects on CMCs ($=2 \mu\text{M}$ for $s = 4, 8,$ and 10 and $3 \mu\text{M}$ for $s = 6$) and a trend toward smaller, more spherical micelles with increasing spacer lengths.²¹ More recently, some of us produced the 16-5-16 MEA Gemini surfactant, characterized its CMC at different temperatures and ionic strengths employing two different methods, and found a CMC value of $2 \mu\text{M}$ at 25°C .²²

As a prerequisite for their use as membrane mimetics, we are characterizing their interaction with well characterized model proteins.^{23,24} Additional analysis of 16-s-16 MEA Gemini surfactants with $s = 4, 5,$ and 6 , which are referred to here individually as GSB, GSP, and GSH, respectively, and as GSX as a group, lead to the complete assignment of their NMR spectra. We also found that they bind DSS, which was used as the internal NMR chemical shift reference.²⁴ We have recently studied their effects on the native state and conformational stability of RNase A and HEWL, two highly stable, well-folded cationic proteins, and found negligible to weak interactions and mild destabilization at acidic to mildly alkaline pH.^{23,24} In contrast, the formation of a series of protein–surfactant complexes was observed above pH 10, where these proteins lose their net positive charge. On the basis of these results, we proposed that hydrophobic interactions and, in particular, favorable electrostatic interactions play crucial roles in complex formation by these surfactants and proteins. To establish if these conclusions are general, we now characterize the

interactions of these Gemini surfactants with an anionic protein, ribonuclease Sa (RNase Sa).

At 96 residues, RNase Sa is the smallest member of the RNase T1 family.²⁵ The contributions of electrostatic interactions²⁶ and particular residues to its conformational stability^{27,28} have been investigated thoroughly. The tertiary structure has been solved both by X-ray crystallographic^{29,30} and NMR solution³¹ techniques, and consists of a β -sheet which is packed on one face by an α -helix and on the other side by loops (Figure 1).

Although RNase Sa contains an excess of negatively charged residues at neutral pH, the “loop face” of the protein contains a region that is dominated by cationic groups which play key roles in the recognition and cleavage of the polyanionic substrate, RNA. RNase Sa cleaves ssRNA specifically on the 3' side of guanosine residues. This enzymatic activity can be assayed to study whether and how Gemini surfactants affect RNase Sa's function.

The main goals of this paper are to investigate the interaction of Gemini surfactants and RNase Sa using NMR and CD spectroscopies to reveal how Gemini surfactants affect the structure, conformational stability, and enzymatic activity of RNase Sa.

EXPERIMENTAL METHODS

Materials. Gemini surfactants were synthesized and purified as previously described from 2-(methylamino)ethanol and *n*-hexadecyl bromide (Aldrich) and 1,4-dibromo butane, 1,5-dibromo pentane, and 1,6-dibromo hexane (Merck).²¹ The products butanediyl-1,4-bis(dimethylhexadecylammonium bromide), pentanediyl-1,5-bis(dimethylhexadecylammonium bromide), and hexanediyl-1,6-bis(dimethylhexadecylammonium bromide) are referred to here individually as GSB, GSP, and GSH, and collectively as GSX. Their composition and purity were confirmed by NMR spectroscopy.²⁴ DSS (Stohler Isotope Chemicals) was used as the internal chemical shift reference at a concentration of $50 \mu\text{M}$. Deuterated water (Cambridge Isotope Laboratories, 99.9% atom D) and NaCl, NaOD, DCl, and deuterated acetic acid (Aldrich, 99.5% atom D) were used for NMR sample preparation. *S. cerevisiae* ssRNA and synthetic poly(A)·poly(U) double stranded RNA were obtained from Sigma.

RNase Sa was produced by expression of a recombinant gene in *E. coli* and purified as previously described.³² The samples used herein were a kind gift of Prof. C. N. Pace (Texas A&M University) to D.V.L. The solution structure of RNase Sa (PDB file: 1C54³¹) and the programs PREKIN and MAGE³³ were used for protein structure analysis and to prepare Figure 1.

Calculation of Net Charge. The fractional charge of individual titratable groups in RNase Sa was calculated at a particular pH value using the Henderson–Hasselbalch equation and the known pK_a values.²⁶ Then, these fractional charges were summed to give the net charge at that pH value. The calculation was repeated at other pH values to determine the net charge as a function of pH.

NMR Spectroscopy. A Bruker 600 MHz instrument, equipped with a cryoprobe and gradients in the Z-axis, was used to record NMR spectra at 25°C . Standard pulse sequences were used to register 1D ^1H , 2D ^1H TOCSY, and NOESY spectra.

CD Spectroscopy. Far UV-CD spectroscopy was performed utilizing a Jasco J-810 spectropolarimeter fitted with a Peltier module for computer-controlled temperature adjust-

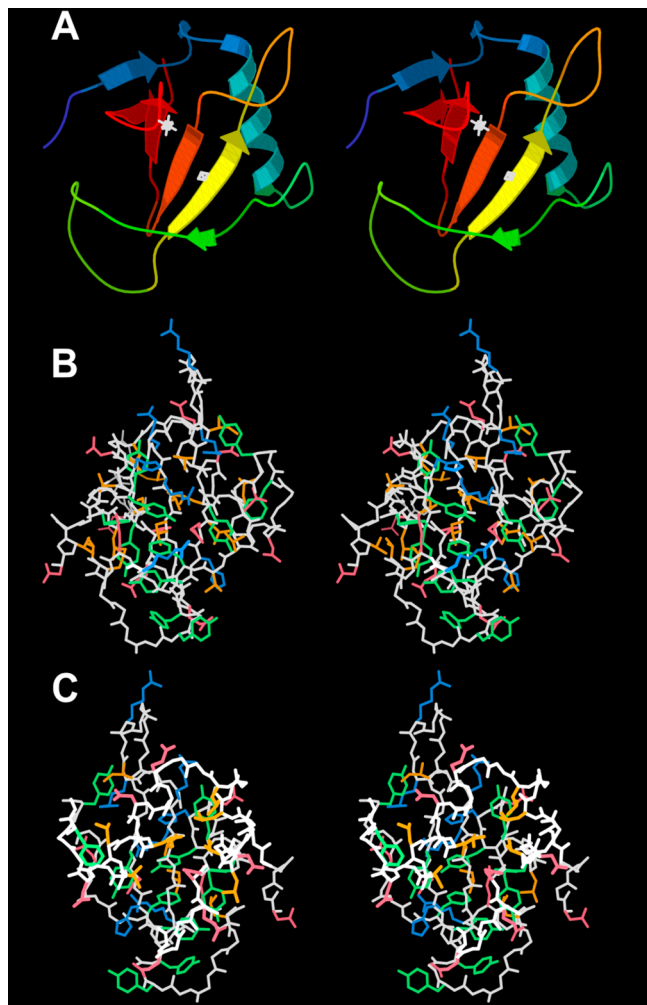


Figure 1. Structure and charged residue content of RNase Sa. (A) Ribbon diagram of RNase Sa in cross-eyed stereo. Starting from the blue N-terminus, the chain follows a rainbow color spectrum to the red C-terminus. The structure consists of a β -sheet packed against a long α -helix on one face (the helix face) and against long loops on the other side (the loop face). White stars mark the side chains of the catalytic residues His 85 (upper left star) and Glu 54 (bottom right star). (B) The loop face of RNase Sa in cross-eyed stereo. The orientation is approximately the same as that in panel A. This face contains several positively charged residues which contribute to RNA binding and cleavage. The main chain is white; Phe and Tyr are green; Val, Leu, and Ile are orange; Asp and Glu are red; His and Arg are blue. For clarity, other residues are not shown. (C) The helix face of RNase Sa in cross-eyed stereo. The orientation shown in panel B has been rotated about 180° around the z-axis. The backbone and side chains are colored as in panel B. This face possesses various negatively charged residues which likely participate in binding to Gemini surfactant.

ment in a 0.1 cm cuvette. Spectra of RNase Sa (1.0 mM) were recorded over an interval of 200–250 nm in the presence or absence of GSX. Typically, four scans, run at a speed of 50 nm/min, were averaged to calculate a final spectrum. Spectra were recorded in 20 mM sodium acetate/acetic acid (Na/HAc) buffer at pH 5.5 or 40 mM glycine buffer at pH 9.0. The same instrument and cuvette were used to monitor the thermal denaturation of RNase Sa at 234 nm, the wavelength where the largest difference in the CD signal of folded and unfolded RNase Sa is observed.³⁴ After denaturation, the sample was

immediately cooled down to measure the reversibility of unfolding. An equation which assumes a two-state native \leftrightarrow denatured unfolding equilibrium and linear dependences of the CD signal of the native and denatured states of the protein on temperature was fit to the data to obtain values of the thermal unfolding midpoint, T_M , the enthalpy change for unfolding ΔH , as previously described.³⁵ The program Kaleidograph (ver. 3.6, Synergy Software) was used for data analysis and preparation of the graphs.

Absorbance Spectra and Enzymatic Assays. The UV spectra of ssRNA (concentration: 0.02 mg/mL) were recorded using a Shimadzu UV spectrometer at 20 °C, alone or in the presence of increasing ratios of RNA:GSH 1:1, 1:2.5, and 1:5 (wt:wt). This corresponds to a concentration of 1.3 mM of nucleotide base (as calculated from the absorbance based on the average composition of A, G, U, and C bases in yeast ssRNA) and 0.12–0.60 mM of GSH. Note that, at a 1:5 ratio (wt:wt) of RNA:GSH, the ratio of negative charges from the RNA and positive charges from GSH is about 1.

RNase Sa's ribonucleolytic activity was measured using an assay, described by Kunitz³⁶ with minor improvements,³⁷ which is based on a decrease in RNA absorbance at 300 nm, which is due to a blue-shift in absorbance of ssRNA upon cleavage at pH 5. In these assays, the ssRNA concentration was much higher, 0.5 mg/mL, than that used to measure the absorbance spectra (*vide supra*). The final RNase Sa concentration was 2.5 μ g/mL = 0.24 μ M. The activity of RNase Sa on ssRNA was measured in the absence or presence of GSH at molar:molar ratios of RNase Sa:GSH ranging from 1 to 5. The data analysis was performed using Kaleidograph.

RESULTS

Detection of Monomeric Gemini Surfactant by NMR.

We previously assigned the NMR spectra of Gemini surfactants and found that many methylene hydrogens resonate between 1.30 and 1.20 ppm.²⁴ Although the observation of ^1H NMR signals typically requires sample concentrations between 50 μ M or higher, the concurrence of many Gemini ^1H in the same chemical shift range led us to test whether very low concentrations of Gemini are detectable by NMR. We found that concentrations of GSX as low as 2–3 μ M are observable by ^1H NMR (Figure 2).

Similar results were found for GSB and GSH (data not shown). As these concentrations are at or just below the CMCs of these Gemini surfactants,^{21,22} we are observing predominately monomeric surfactant molecules and not micelles. As the GSP concentration is increased, the resonances arising from the DSS methylene hydrogens at 2.9, 1.8, and 0.6 ppm broaden and the signal from the trimethyl moiety shifts 0.04 ppm downfield. These results corroborate previous measurements made with higher concentrations of GSH where these changes were attributed to DSS binding to GSH. The current result leads us to propose that DSS binds to Gemini micelles and that the stoichiometry of the DSS:GSX complex is higher than 1.

Interaction of Gemini Surfactants and RNase Sa Studied by NMR Spectroscopy. We used NMR spectroscopy to test whether monomeric Gemini surfactants are capable of interacting with RNase Sa. Addition of RNase Sa to solutions of GSX at concentrations (2–3 μ M) where the surfactant monomer is the chief species at pH* 5.4 caused the ^1H Gemini methylene peak to disappear (Figure 3).

The observed loss of signal can be attributed to the formation of a large Gemini surfactant–RNase Sa complex

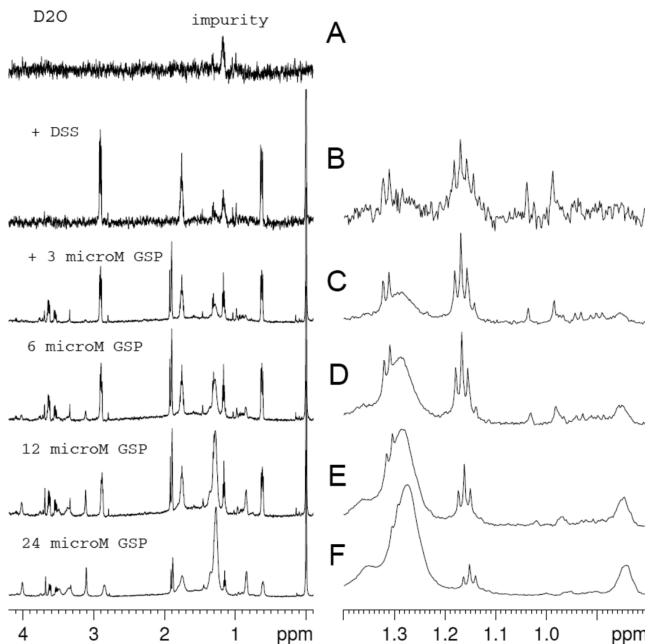


Figure 2. NMR observation of micromolar concentrations of monomeric gemini surfactants. Left: From top to bottom, (A) 1D ¹H NMR spectra of D₂O; (B) D₂O and 50 μM DSS; (C) D₂O, 50 μM DSS, and 3 μM GSP; (D) D₂O, 50 μM DSS, and 6 μM GSP; (E) D₂O, 50 μM DSS, and 12 μM GSP; (F) D₂O, 50 μM DSS, and 24 μM GSP. In D₂O (top panel), the only peak seen is an impurity peak at 1.17 ppm. Upon addition of DSS (next panel), a sharp intense peak at 0.00 ppm (arising from the trimethyl moiety), triplets at 2.91 and 0.63 ppm, as well as a multiplet at 1.76 ppm (from the three methylene groups) appear. Upon addition of just 3 μM GSP, weak but detectable peaks coming from the methylene and methyl groups at 1.29 and 0.86 ppm, respectively, appear and become more intense at higher concentrations (lower panels). Right: Zoom view which highlights the increase of the GSP methylene and methyl peak at 1.26 and 0.84 ppm, respectively.

with a significantly slowed tumbling in solution, altered correlation time, and severe NMR line broadening. This indicates that monomeric Gemini surfactants bind to RNase Sa.

Next, we investigated the pH dependence of the interaction between RNase Sa and Gemini surfactants by NMR. Upon mixing equivalent amounts of RNase Sa and GSP, each of which had been dissolved separately in pH 5.0 buffer, a white precipitate formed. The 1D ¹H NMR spectrum of this sample is essentially equivalent to that of a sample of RNase Sa recorded under the same conditions. This suggests that the aggregation complex contains more than one equivalent of GSP per RNase Sa, leaving excess RNase Sa in solution. The precipitate remained visible at pHs 3.89, 4.61, 5.92, 6.64, and 8.32 but disappeared, yielding a transparent solution at pHs 3.30, 3.02, and 2.25. Under these acidic conditions, the 1D ¹H and 2D TOCSY and NOESY NMR spectra of this sample at pH 3.30 reveal signals of both substances and no intermolecular NOEs could be assigned unambiguously (Figure 4A,B).

This suggests that the precipitate completely dissolved and that there are no detectable contacts between RNase Sa and GSP at pH 3.30 or below. The observed pH dependence suggests that RNase Sa's capacity to interact with GSX depends on its net charge. The contribution of different types of residues and the net charge of RNase Sa is shown as a function of pH in Figure 4C. The overall charge on the protein is positive at acidic pH, passes zero near pH 4.5, and then becomes negative

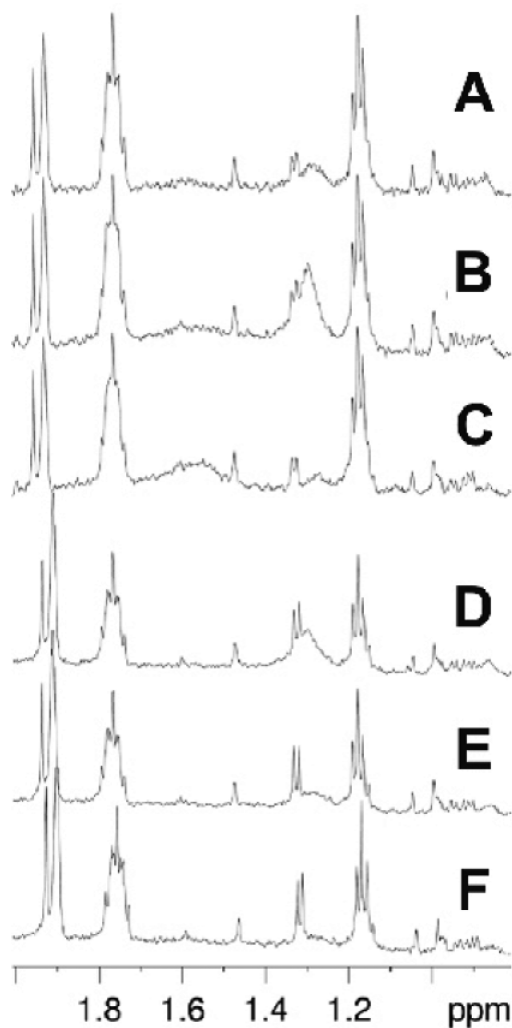


Figure 3. RNase Sa binds monomeric gemini surfactants. (A) 1D ¹H NMR spectrum of 10 mM acetate/acetic acid buffered D₂O solution, pH* 5.4. Peaks from acetate (1.92 ppm), DSS (multiplet at 1.77 ppm), and an impurity (1.18 ppm) can be seen. (B) Addition of 2.0 μM GSH leads to a new peak at 1.3 ppm, arising from the ¹H of the methylene groups. (C) Disappearance of the methylene peak upon addition of RNase Sa to a final concentration of 0.95 μM. (D) Spectrum of 3.0 μM GSP in the same buffer as panel A. (E) The peak in panel D is significantly reduced upon the addition of 0.16 μM RNase Sa. (F) Disappearance of the GSP ¹H methylene peak in the presence of 0.31 μM RNase Sa.

at higher pH. RNase Sa and GSP form an insoluble complex when the net charge on the protein is less than +1 and become soluble when its net charge is higher than +4. As Asp and Glu residues titrate over this pH range, these residues, or a subset of them, are likely to play key roles in the RNase Sa-GSP recognition event and aggregate formation. The helical face of RNase, which is dominated by anionic groups (Figure 1C), is likely to participate in GSP recognition.

Next, we utilized NMR spectroscopy to explore the stoichiometry of the RNase Sa · Gemini surfactant complex. In the absence of surfactant at pH* 5.5 and 25 °C, RNase Sa shows a wide chemical shift peak dispersion typical of a well-folded protein (Figure 5A).

Addition of subequivalent amounts of GSP, where the surfactant:protein (S:P) ratio is 1.0, produces visible precipitate and a loss of NMR signal intensity without significant chemical

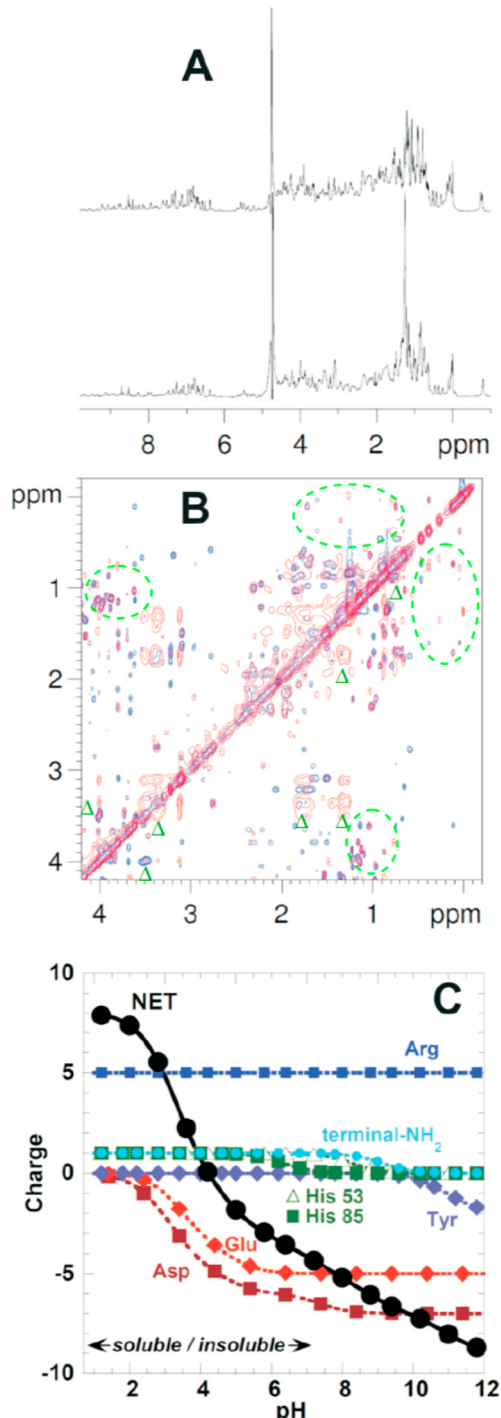


Figure 4. pH dependence of the interaction between RNase Sa and Gemini surfactants. (A) 1D ^1H NMR spectra in D_2O of RNase Sa and GSP (molar ratio 1:1). At pH 5.6 (top spectrum), a white precipitate is visible and the NMR spectrum shows RNase Sa but no signals characteristic of GSP. At pH 3.3, the precipitate dissolves and an intense peak near 1.3 ppm coming from the methylene groups of GSP appears (bottom spectrum). (B) 2D ^1H TOCSY (blue signals, mixing time 60 ms) and ^1H NOESY (red signals, mixing time 150 ms) of the 1:1 RNase Sa and GSP mixture at pH* 3.3, 25 °C in D_2O . Some representative signals of GSP are marked with green triangles, and some peaks arising from folded RNase Sa are circled with green ellipses. (C) The contribution of the titrating residues to the net charge of RNase Sa. Note that RNase Sa-GSX mixtures become soluble at acidic pH when the protein's net charge is over +4.

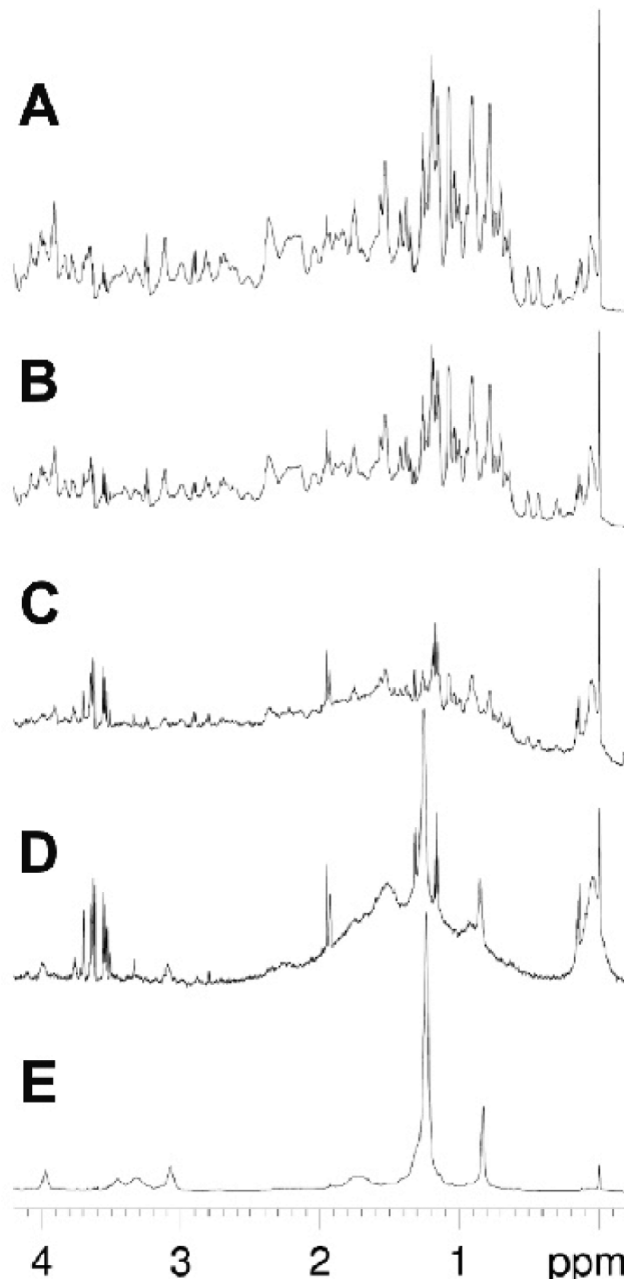


Figure 5. Stoichiometry of RNase Sa · GSX complex. 1D ^1H NMR spectra of 96 μM RNase Sa alone (A) and in the presence of 96 μM (B), 168 μM (C), 227 μM (D), and 343 μM (E) GSP. Spectra were recorded at 25.0 °C, pH* 5.5 with 10 mM deuterated acetic acid/sodium acetate buffer. The fine signals at 3.5–3.8 ppm are impurities. Their intensities do not change, but they become prominent in panels C and D where the vertical scale has been magnified due to the low intensity of the RNase Sa and GSP signals.

shift or line width changes (Figure 5B). Upon further additions of GSP, to just below the equivalence point (S:P = 1.8), the spectra reveal small native RNase Sa resonances superimposed on broader signals which could correspond to proteins which have formed a large complex with GSP (Figure 5C). At higher concentrations of GSP, S:P = 2.5, slightly above the equivalence point, only broad RNase Sa signals and narrow GSP peaks are seen (Figure 5D). At still higher concentrations of GSP, S:P=4.5, the RNase Sa resonances have vanished (Figure 5E).

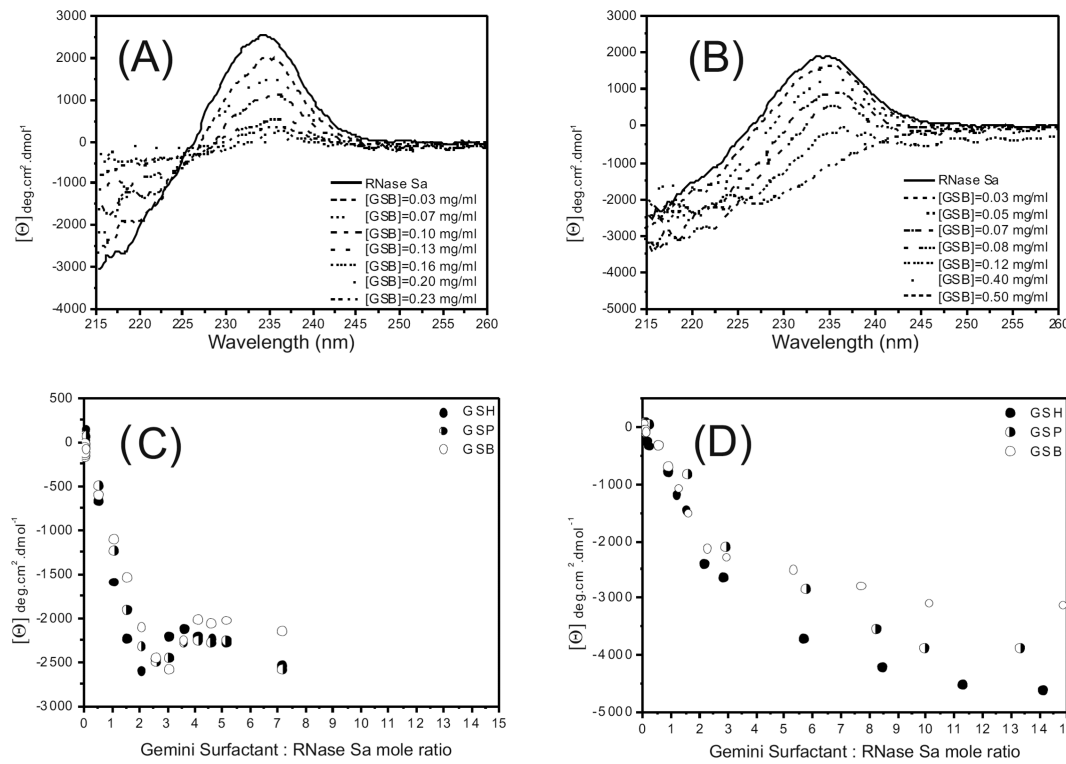


Figure 6. Interaction of Gemini surfactants with RNase Sa monitored by far UV-CD spectroscopy. (A and B) Far UV-CD spectra of RNase Sa alone and in increasing amounts of GSB at pH 5.5 (A) and pH 9.0 (B). The maximum at 234 nm, which arises from fixed aromatic groups in the folded protein, decreases as the protein aggregates and unfolds in the presence of GSB. (C and D) The dependence of the CD signal at 234 nm at increasing ratios of GSX:RNase A at pH 5.5 (C) and pH 9.0 (D).

These experiments were repeated with GSB and GSH and yielded similar results (data not shown).

Circular Dichroism Spectroscopy. CD spectroscopy was utilized to quantitate the interaction between Gemini surfactants and RNase Sa more precisely. The far UV-CD spectrum of RNase Sa is rather unusual in that it is dominated by a positive band that arises from aromatic side chains being in a fixed conformation within the folded protein.^{38,34} When titrated with GSB, the CD band indicative of native-state RNase Sa decreases sharply at pH 5.5, reaching a minimum at a surfactant:protein (S:P) ratio of about 2.5:1 (Figure 6A).

Interestingly, at higher concentrations of Gemini surfactant, a partial recovery of the native CD band is observed. Similar spectral changes were seen for GSP and GSH (data not shown). Despite the overall similarity, it could be observed that Gemini surfactant with the longest spacer, GSH, appears to be slightly more effective at decreasing the native CD signal of RNase Sa. In contrast, GSB, which has the shortest spacer, seems to be a little more potent at inducing the partial recovery of the native CD band (Figure 6C).

Changes in the CD spectrum of RNase Sa upon GSX titration were also followed at pH 9.0 (Figure 6B). Like at pH 5.5, Gemini surfactants produce a loss of the native RNase Sa far UV-CD band, except that the CD signal at 234 nm continues to decrease at S:P ratios higher than 2.5. Higher ratios of surfactants are required to induce this change at pH 9.0. In fact, at pH 9.0, the loss of CD signal is still not complete at GSX to RNase Sa ratios of 10:1 (Figure 6D). This suggests that more surfactant binds RNase Sa at pH 9.0 than pH 5.5; this is reasonable considering that the protein bears more negative charge at alkaline pH (Figure 4B).

Thermal Denaturation of RNase Sa Followed by CD.

The effect of Gemini surfactants on the conformational stability of RNase Sa was studied by thermal denaturation monitored by CD at 234 nm. RNase Sa was found to be more stable at pH 5.5 than 9.0 in agreement with previous results³⁴ (Figure 7A,B).

At low GSX:RNase Sa ratios, up to about 2:1, part of the CD signal arising from RNase Sa is lost, but otherwise the thermal unfolding transitions resemble those of RNase Sa in the absence of Gemini surfactant (Figure 7). Similar observations were obtained for the three different surfactants. These results can be attributed to the formation of a Gemini-RNase Sa aggregate which apparently does not equilibrate or equilibrates very slowly with the excess of unassociated RNase Sa remaining in solution. This excess RNase Sa then undergoes thermal denaturation without being affected by the presence of aggregates. At S:P ratios between 2 and 3, very little CD signal change can be observed. This suggests that, at these ratios, essentially all the RNase Sa has formed an aggregate with Gemini surfactant. As the surfactant:protein ratio increases to 5, an apparent thermal unfolding transition, with a reduced $T_{M^{\circ}}$, is observed. On the basis of this result, we propose that, in higher relative concentrations of Gemini surfactant, RNase Sa can adopt a partially folded state, which may or may not be native-like, which shows a reduced stability toward thermal denaturation.

RNase Sa Can Cleave ssRNA Despite the Presence of GSH. A spectroscopic assay was employed to study the effects of GSH on RNase Sa's enzymatic activity. Prior to these measurements, experiments were carried out to determine if GSH binds to the RNA substrate. UV spectra show a marked increase in extinction when Gemini surfactants are added to a solution of yeast ssRNA (Figure 8A).

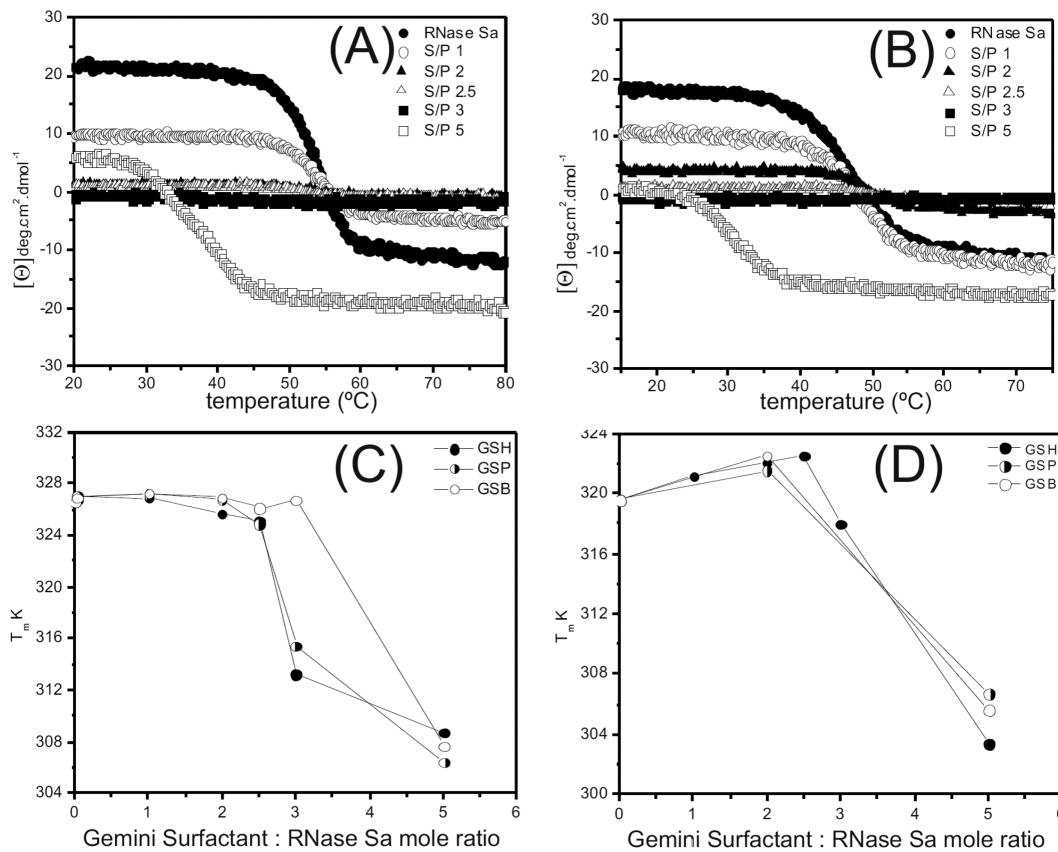


Figure 7. Higher ratios of Gemini surfactants destabilize RNase Sa. Thermal denaturation of RNase Sa in the presence of increasing ratios of GSH monitored at 234 nm by CD at pH 5.5 (A) and pH 9.0 (B). S/P means surfactant/protein ratio. The thermal denaturation midpoints (T_m) are plotted as a function of GSX at pH 5.5 (C) and pH 9.0 (D).

The samples also become visibly turbid. This clearly indicates that RNA and Gemini surfactants can form a large complex. Similar results were also observed for poly(A)-poly(U), a double stranded synthetic RNA. These interactions are not surprising, considering that both RNA and Gemini surfactants contain hydrophobic moieties and complementary charges. These interactions have been proposed previously to govern the binding of simple cationic surfactants and nucleic acids.³⁹ Indeed, it was recognized early on that the structure and charge of Gemini surfactants could be specifically tailored to enhance their nucleic acid binding efficiency as nonviral vectors for gene therapy.⁴⁰ Although the stoichiometry of this ssRNA-Gemini complex is difficult to ascertain due to the heterogeneity of the former, the increase in extinction seems to level off above 2.5 equiv of GSX:ssRNA (Figure 8A, inset).

Despite the presence of GSH, RNase Sa is still able to recognize and cleave the ssRNA, as indicated by a decrease in extinction upon addition of the protein (Figure 8B). No absorbance changes were observed when RNase Sa is added to a solution of poly(A)-poly(U), with or without GSH. This is consistent with the known specificity of RNase Sa for G bases in ssRNA. The dependence of the observed reaction rate of RNase Sa on ssRNA and the overall extent of the cleavage on the GSH ratio are shown in Figure 8C. There is a slight trend toward slower reaction rates and less complete reactions at higher GSH ratios; however, the presence of the surfactant did not impede RNA cleavage by RNase Sa. In an additional experiment, RNase Sa was first incubated with GSH, and then, these aggregates were added to a solution of ssRNA. Hydrolysis

of RNA was still observed, though less extensive, and the observed cleavage rate was slower (Figure 8C).

DISCUSSION

The results reported here show that the ability of folded RNase Sa to interact with cationic Gemini depends on the protein's charge. The interactions and aggregation observed at alkaline and neutral pH, where the protein is anionic, disappear at pH values below 4, where the protein carries a net positive charge. These results are consistent with those obtained for RNase A and HEWL, two highly stable cationic proteins.²⁴ On this basis, we conclude that cationic Gemini surfactants will bind, in general, to proteins when they carry a negative charge.

In addition, the thermal denaturation experiments monitored by CD reveal that these Gemini surfactants can also interact with unfolded RNase Sa. This union is somewhat stronger than that occurring between folded RNase Sa and Gemini surfactants, and thus, Gemini surfactants tend to favor unfolding. These interactions are not strong enough to unfold RNase Sa under benign conditions but will maintain RNase Sa in a denatured state once it is heat-unfolded. These results are also in line with those observed previously for RNase A and HEWL.²⁴

The micelles of simple surfactants, like SDS, have frequently been employed as membrane mimetics for biophysical studies such as the structural characterization of peripheral membrane proteins by NMR spectroscopy (see, for example, ref 41). Nevertheless, the interpretation of these experiments is complicated by the presence of significant interactions between

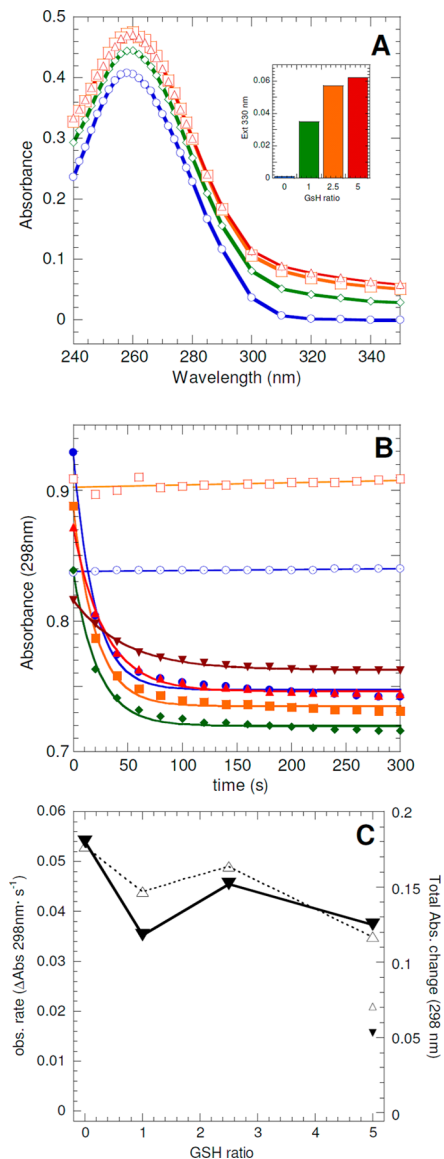


Figure 8. Complex formation between GSH and RNA or GSH and RNase Sa does not prevent RNase Sa from cleaving RNA. (A) Absorbance spectra of yeast ssRNA alone (blue open circles) or in the presence of increasing ratios (wt:wt) of GSH: 1 = green open diamonds; 2.5 = orange open squares; 5 = red open triangles. Inset: The turbidity due to large aggregates is plotted as the extinction (apparent absorbance) at 330 nm. (B) Cleavage of ssRNA followed by absorbance changes at 298 nm, the absence or presence of varying ratios of GSH (ratios here are molar:molar::GSH:RNase Sa). RNA alone = blue open circles; RNA + 2.5× GSH = orange open squares. The blue and orange lines represent the least-squares fit of a linear equation to the data. RNA + RNase Sa = blue filled circles; (RNA + 1 equiv of GSH), then + RNase Sa = green filled diamonds; (RNA + 2.5 equiv of GSH), then + RNase Sa = orange filled squares; (RNA + 5 equiv of GSH), then + RNase Sa = bright red filled triangles; (5 equiv of GSH + RNase Sa), then + RNA = maroon filled inverted triangles. The curves represent the least-squares fit of an exponential equation ($\text{Abs}(t) = \Delta\text{Abs} \times e^{-kt} + \text{Abs}\infty$) to each data set. (C) The observed reaction rate (open triangles, left y-axis) and overall absorbance change (filled inverted triangles, right y-axis) obtained from the data fits in part B are shown. The lines connecting the points are meant to guide the eye; they do not represent a least-squares fit. The small triangles at GSH = 5 show the results of the experiment where GSH and RNase Sa were combined prior to the addition of RNA.

the protein and surfactant monomers, since surfactant monomers and micelles can exert different effects on protein structure.⁴² These interactions can be especially troublesome, as the surfactant monomer's hydrophobic aliphatic moiety may well bind to the protein of interest, and in a physiological setting, the aliphatic components of membrane lipids are not accessed by peripheral membrane proteins. Compared to simple surfactants, Gemini surfactants have low μM CMCs and slow monomer micelle kinetics and these characteristics have been touted by Gemini surfactant advocates as important advantages.⁷ These advantages have stimulated a good deal of interest in utilizing Gemini surfactants as membrane mimetics for biophysical studies and as delivery vehicles for gene therapy.^{17–20,40,43,44} Whereas it is generally thought that Gemini surfactant monomers are too low in concentration to interact significantly with proteins, this assumption has been rarely tested. In the one study we are aware of, interactions between protein and an anionic Gemini surfactant in its monomeric form were detected by conductivity measurements.⁴⁵

Here, we have used high sensitivity NMR measurements to observe via spectroscopy for the first time to our knowledge the interaction between *monomeric* cationic Gemini surfactant monomers and a protein, which leads to the formation of a high molecular weight aggregate. This discovery is important because it means that we cannot ignore, *a priori*, possible interactions between cationic Gemini surfactant monomers and proteins just because the former have a low CMC, even for this 16-s-16 MEA series of Gemini surfactants which have very low CMCs. Currently, a new class of Gemini surfactants in which the aliphatic groups are covalently linked to essentially eliminate the formation of monomer is under development by Abe and co-workers.⁴⁶ In our opinion, this is a promising approach to avoid the complications arising from the interactions of surfactant monomers and proteins.

Finally, our observation of interactions between Gemini surfactants and RNA means that similar interactions will occur between Gemini surfactants as vehicles for gene therapy and their nucleic acid "cargo". However, the results of our enzyme activity measurements show that the interactions between Gemini surfactants and RNA and Gemini surfactants and RNase Sa are too weak to prevent RNase Sa from binding and cleaving RNA. This is logical considering that the evolution has honed RNase Sa to have an elevated affinity and a high specificity for ssRNA. Gemini surfactant micelles, like those simple cationic surfactants and certain intrinsically disordered cationic proteins, could speed nucleic acid complementation by providing a hub for interactions.^{47,48} Nevertheless, the interactions between Gemini surfactants and nucleic acids could be significant when the affinity of the nucleic acid's partner is weak and can not surmount that of the Gemini surfactant. This possibility should be borne in mind when utilizing Gemini surfactants for gene delivery.

CONCLUSIONS

Here, electrostatic interactions have been shown to govern the interaction between folded RNase Sa and a series of cationic Gemini surfactants with remarkably low CMCs. Despite being present at minute concentrations, just 2–3 μM , surfactant monomers bind RNase Sa. Gemini surfactants can destabilize folded RNase Sa by preferentially binding to the denatured state. These Gemini surfactants also bind RNA, but this

association does not prevent RNase Sa from recognizing and cleaving RNA.

AUTHOR INFORMATION

Corresponding Author

*E-mail: dlaurens@iqfr.csic.es. Phone: +34 (91) 745-9543. Fax: +34 (91) 564-2431.

Notes

The authors declare no competing financial interest.

ACKNOWLEDGMENTS

This work was supported by the University of Isfahan and grants from the Spanish MICINN (CTQ2010-21567-C02-02) and MINECO (SAF2013-49179-C2-2R). We thank Prof. C. Nick Pace (Texas A&M University) for the generous gift of RNase Sa.

ABBREVIATIONS

CMC, critical micelle concentration; DSS, sodium 2,2-dimethyl-2-silapentane-sulfonate; GSB, butanediyl-1,4-bis(dimethylhexadecylammonium bromide); GSP, pentanediyl-1,5-bis(dimethylhexadecylammonium bromide); GSH, hexanediyyl-1,6-bis(dimethylhexadecylammonium bromide); GSX, the gemini surfactants GSB, GSP, and GSH as a group; HEWL, hen egg white lysozyme; MEA, monoethanolamine; NMR, nuclear magnetic resonance; pH*, the pH meter reading in D₂O without correction for the isotope effect; SDS-PAGE, sodium dodecyl sulfate polyacrylamide gel electrophoresis; ssRNA, single stranded RNA

REFERENCES

- (1) Debey, P. Light Scattering in Soap Solutions. *J. Phys. Colloid Chem.* **1949**, *53*, 1–8.
- (2) Tanford, C. Thermodynamics of Micelle Formation: Prediction of Micelle Size and Size Distribution. *Proc. Natl. Acad. Sci. U. S. A.* **1974**, *71*, 1811–1815.
- (3) Tanford, C. Micelle Shape and Size. *J. Phys. Chem.* **1972**, *76*, 3020–3024.
- (4) Tanford, C. *The Hydrophobic Effect*; Wiley: New York, 1973.
- (5) Laemmli, U. K. Cleavage of Structural Proteins During the Assembly of the Head of Bacteriophage T4. *Nature* **1970**, *227*, 680–685.
- (6) Popot, J. L.; Althoff, T.; Bagnard, D.; Banères, J. L.; Bazzacco, P.; Billon-Denis, E.; Catoire, L. J.; Champeil, P.; Charvolin, D.; Cocco, M. J. Amphipols from A to Z. *Annu. Rev. Biophys.* **2011**, *40*, 379–408.
- (7) Menger, F. M.; Keiper, J. S. Gemini Surfactants. *Angew. Chem., Int. Ed.* **2000**, *39*, 1906–1920.
- (8) Sakai, K.; Sakai, H.; Abe, M. Recent Advances in Gemini Surfactants: Oleic Acid-Based Gemini Surfactants and Polymerizable Gemini Surfactants. *J. Oleo Sci.* **2010**, *60*, 159–163.
- (9) De, S.; Aswal, V. K.; Goyal, P. S.; Bhattacharya, S. Role of Spacer Chain Length in Dimeric Micellar Organization: Small Angle Neutron Scattering and Fluorescence Studies. *J. Phys. Chem.* **1996**, *100*, 11664–11671.
- (10) De, S.; Aswal, V. K.; Goyal, P. S.; Bhattacharya, S. Novel Gemini Micelles from Dimeric Surfactants with Oxyethylene Spacer Chain. Small Angle Neutron Scattering and Fluorescence Studies. *J. Phys. Chem. B* **1998**, *102*, 6152–6160.
- (11) De, S.; Aswal, V. K.; Goyal, P. S.; Bhattacharya, S. Small-Angle Neutron Scattering Studies of Different Mixed Micelles Composed of Dimeric and Monomeric Cationic Surfactants. *J. Phys. Chem. B* **1997**, *101*, 5639–5645.
- (12) Haldar, J.; Aswal, V. K.; Goyal, P. S.; Bhattacharya, S. Molecular Modulation of Surfactant Aggregation in Water: Effect of the Incorporation of Multiple Headgroups on Micellar Properties. *Angew. Chem., Int. Ed.* **2001**, *40*, 1228–1232.
- (13) Bhattacharya, S.; De, S. Vesicle Formation from Dimeric Surfactants through Ion-Pairing. Adjustment of Polar Headgroup Separation Leads to Control over Vesicular Thermotropic Properties. *J. Chem. Soc., Chem. Commun.* **1995**, *651*–652.
- (14) Bhattacharya, S.; De, S. Vesicle Formation from Dimeric Ion-Paired Amphiphiles. Control over Vesicular Thermotropic and Ion-Transport Properties as a Function of Intra-Amphiphilic Headgroup separation. *Langmuir* **1999**, *15*, 3400–3410.
- (15) Bhattacharya, S.; Biswas, J. Role of Spacer Lengths of Gemini Surfactants in the Synthesis of Silver Nanorods in Micellar Media. *Nanoscale* **2011**, *3*, 2924–2930.
- (16) Datta, S.; Biswas, J.; Bhattacharya, S. How Does Spacer Length of Imidazolium Gemini Surfactants Control the Fabrication of 2D-Langmuir Films of Silver-Nanoparticles at the Air-water Interface? *J. Colloid Interface Sci.* **2014**, *430*, 85–92.
- (17) Bajaj, A.; Kondaiah, P.; Bhattacharya, S. Synthesis and Gene Transfer Activities of Novel Serum Compatible Cholesterol-Based Gemini Lipids Possessing Oxyethylene-Type Spacers. *Bioconjugate Chem.* **2007**, *18*, 1537–1546.
- (18) Muñoz-Úbeda, M.; Misra, S. K.; Barrán-Berdón, A. L.; Aicart-Ramos, C.; Sierra, M. B.; Biswas, J.; Kondaiah, P.; Junquera, E.; Bhattacharya, S.; Aicart, E. Why is Less Cationic Lipid Required to Prepare Lipoplexes from Plasmid DNA than Linear DNA in Gene Therapy? *J. Am. Chem. Soc.* **2011**, *133*, 18014–18017.
- (19) Muñoz-Úbeda, M.; Misra, S. K.; Barrán-Berdón, A. L.; Datta, S.; Aicart-Ramos, C.; Castro-Hartmann, P.; Kondaiah, P.; Junquera, E.; Bhattacharya, S.; Aicart, E. How Does the Spacer Length of Cationic Gemini Lipids Influence the Lipoplex Formation with Plasmid DNA? Physicochemical and Biochemical Characterizations and their Relevance in Gene Therapy. *Biomacromolecules* **2012**, *13*, 3926–3937.
- (20) Misra, S. K.; Naz, S.; Kondaiah, P.; Bhattacharya, S. A Cationic Cholesterol Based Nanocarrier for the Delivery of p53-EGFP-C3 Plasmid to Cancer Cells. *Biomaterials* **2014**, *34*, 1334–1346.
- (21) Sharma, V.; Borse, M.; Aswal, V. K.; Pokhriyal, N. K.; Joshi, J. V.; Goyal, P. S.; Devi, S. Synthesis, characterization, and SANS studies of Novel Alkanediyl-alpha,omega-bis(hydroxyethylmethylhexadecylammonium bromide) Cationic Gemini Surfactants. *J. Colloid Interface Sci.* **2004**, *277*, 450–455.
- (22) Zarganian, R.; Bordbar, A. K.; Amiri, R.; Tamannaei, M.; Khosropour, A. R.; Mohammadpoor-Baltork, I. Micellization of Pentanediyl-1,5-bis(hydroxyethylmethyl hexadecylammonium bromide) as a Cationic Gemini Surfactant in Aqueous Solutions: Investigation using Conductometry and Fluorescence Techniques. *J. Solution Chem.* **2011**, *40*, 921–928.
- (23) Amiri, R.; Bordbar, A. K.; Laurents, D. V.; Khosropour, A. R.; Baltork, I. M. Thermal Stability and Enzymatic Activity of RNase A in the Presence of Cationic Gemini Surfactants. *Int. J. Biol. Macromol.* **2011**, *50*, 1151–1157.
- (24) Amiri, R.; Bordbar, A. K.; García Mayoral, M. F.; Khosropour, A. R.; Mohammadpoor-Baltork, I.; Menendez, M.; Laurents, D. V. Interactions of Gemini Surfactants with Two Model Proteins: NMR, CD and Fluorescence Spectroscopies. *J. Colloid Interface Sci.* **2012**, *269*, 245–255.
- (25) Irie, M. RNase T1/RNase T2 Family RNases. In *Ribonucleases: Structures and Functions*; D'Alessio, G., Riordan, J. F., Eds.; Academic Press: New York, 1997; pp 101–130.
- (26) Laurents, D. V.; Huyghues-Despointes, B. M.; Bruix, M.; Thurlkill, R. L.; Schell, D.; Newsom, S.; Grimsley, G. R.; Shaw, K. L.; Trevino, S.; Rico, M. Charge-charge Interactions are Key Determinants of the pK Values of Ionizable Groups in Ribonuclease Sa (pI=3.5) and a Basic Variant (pI=10.2). *J. Mol. Biol.* **2003**, *325*, 1077–1092.
- (27) Laurents, D. V.; Gorman, P. M.; Guo, M.; Rico, M.; Chakrabarty, A.; Bruix, M. Alzheimer's Abeta40 studied by NMR at Low pH Reveals that Sodium 4,4-Dimethyl-4-Silapentane-1-Sulfonate (DSS) Binds and Promotes Beta-Ball Oligomerization. *J. Biol. Chem.* **2005**, *280*, 3675–3685.

- (28) Trevino, S. R.; Gokulan, K.; Newsom, S.; Thurlkill, R. L.; Shaw, K. L.; Mitkevich, V. A.; Makarov, A. A.; Sacchettini, J. C.; Scholtz, J. M.; Pace, C. N. Asp79 Makes a Large, Unfavorable Contribution to the Stability of RNase Sa. *J. Mol. Biol.* **2005**, *354*, 967–978.
- (29) Sevcik, J.; Hill, C. P.; Dauter, Z.; Wilson, K. S. Complex of Ribonuclease from *Streptomyces aureofaciens* with 2'GMP at 1.7 Å Resolution. *Acta Crystallogr., Sect. D* **1993**, *49*, 257–271.
- (30) Sevcik, J.; Lamzin, V. S.; Dauter, Z.; Wilson, K. S. Atomic Resolution Data Reveal Flexibility in the Structure of RNase Sa. *Acta Crystallogr., Sect. D* **2002**, *58*, 1307–1313.
- (31) Laurens, D. V.; Pérez-Cañadillas, J. M.; Santoro, J.; Rico, M.; Schell, D.; Pace, C. N.; Bruix, M. Solution Structure and Dynamics of Ribonuclease Sa. *Proteins: Struct., Funct., Genet.* **2001**, *44*, 200–211.
- (32) Hebert, E. J.; Grimsley, G. R.; Hartley, R. W.; Horn, G.; Schell, D.; Garcia, S.; Both, V.; Sevcik, J.; Pace, C. N. Purification of Ribonucleases Sa, Sa2 and Sa3 after Expression in *Escherichia coli*. *Protein Expression Purif.* **1997**, *11*, 162–168.
- (33) Richardson, D. C.; Richardson, J. S. The Kinemage: A Tool for Scientific Communication. *Protein Sci.* **1992**, *1*, 3–9.
- (34) Pace, C. N.; Hebert, E. J.; Shaw, K. L.; Schell, D.; Both, V.; Krajcikova, D.; Sevcik, J.; Wilson, K. S.; Dauter, Z.; Hartley, R. W. Conformational Stability and Thermodynamics of Folding of Ribonucleases Sa, Sa2 and Sa3. *J. Mol. Biol.* **1998**, *279*, 271–286.
- (35) Pace, C. N.; Scholtz, J. M. Measuring the conformational stability of a protein. In *Protein Structure*; Creighton, T. E., Ed.; Oxford University Press: Oxford, U.K., 1997; pp 253–259.
- (36) Kunitz, M. A Spectrophotometric Method for the Measurement of Ribonuclease Activity. *J. Biol. Chem.* **1946**, *164*, 563–568.
- (37) Pulido, D.; López-Alonso, J. P.; Marchán, V.; González, C.; Grandas, A.; Laurens, D. V. Preparation of Ribonuclease S Domain-Swapped Dimers Conjugated with DNA and PNA: Modulating the Activity of Ribonucleases. *Bioconjugate Chem.* **2008**, *19*, 263–270.
- (38) Woody, R. W. Circular Dichroism. *Methods Enzymol.* **1995**, *246*, 34–71.
- (39) Liu, R.; Yang, J.; Sun, C.; Wu, X.; Su, B. Study on the Interaction Between Nucleic Acids and Cationic Surfactants. *Colloids Surf., B* **2004**, *34*, 59–63.
- (40) McGregor, C.; Perrin, C.; Monck, M.; Camilleri, P.; Kirby, A. J. Rational Approaches to the Design of Cationic Gemini Surfactants for Gene Delivery. *J. Am. Chem. Soc.* **2001**, *123*, 6214–6220.
- (41) Chandra, S.; Chen, X.; Rizo, J.; Jahn, R.; Sudhof, T. C. A Broken Helical Domain in Folded alpha-Synuclein. *J. Biol. Chem.* **2003**, *278*, 15313–15318.
- (42) Sun, C.; Yang, J.; Wu, X.; Huang, X.; Wang, F.; Liu, S. Unfolding and Refolding of Bovine Serum Albumin Induced by Cetylpyridinium Bromide. *Biophys. J.* **2005**, *88*, 3518–3524.
- (43) Kumar, M.; Jinturkar, K.; Yadav, M. R.; Misra, A. Gemini Amphiphiles: A Novel Class of Mon-Viral Gene Delivery Vectors. *Crit. Rev. Ther. Drug Carrier Syst.* **2010**, *27*, 237–278.
- (44) Donkuru, M.; Budea, I.; Wettig, S.; Verrall, R.; Elsbahy, M.; Foldvari, M. Advancing Nonviral Gene Delivery: Lipid- and Surfactant-Based Nanoparticle Design Strategies. *Nanomedicine* **2010**, *5*, 1103–1127.
- (45) Faustino, C. M. C.; Calado, A. R. T.; Garcia-Rio, L. Gemini Surfactant-Protein Interactions: Effect of pH, Temperature and Surfactant Stereochemistry. *Biomacromolecules* **2009**, *10*, 2508–2514.
- (46) Abe, M.; Koike, T.; Nishiyama, H.; Sharma, S. C.; Tsubone, K.; Tsuchiya, K.; Sakai, K.; Sakai, H.; Shchipunov, Y. A.; Schmidt, J. Polymerized Assemblies of Cationic Gemini Surfactants in Aqueous Solution. *J. Colloid Interface Sci.* **2009**, *330*, 250–253.
- (47) Pontius, B. W.; Berg, P. Rapid Renaturation of Complementary DNA Strands Modified by Cationic Detergents: A Role for High Probability Binding Domains in Enhancing the Kinetics of Molecular Assembly Processes. *Proc. Natl. Acad. Sci. U. S. A.* **1991**, *88*, 8237–8241.
- (48) Pontius, B. W. Close Encounters: Why Unstructured, Polymeric Domains Can Increase Rates of Specific Macromolecular Association. *Trends Biochem. Sci.* **1993**, *18*, 181–186.